The relation

$$\lim_{Y\to 0^+}(\partial I/\partial X)=\lim_{Y\to 0^-}(\partial I/\partial X)$$

comes from Eqs. (4) and (5) and can also be proved following Refs. 4 and 6. Note that Eqs. (4) and (5) are identical and represent a single equation for the symmetric part of the velocity only. The second requisite independent equation may be obtained by differentiating the integral equation for $\Phi(X,Y,Z)$ with respect to Y along with the tangency boundary condition at the wing surface. The problem is thus reduced to the solution of the coupled pair of integral equations, and an iteration is necessary to solve them.

An alternative formulation of the integral equations (1) can be obtained as follows. By the application of Green's theorem, the three-dimensional transonic equation for the reduced perturbation potential Φ may be converted to the following integral equation, as shown in detail by Klunker.[1]

$$\Phi(X,Y,Z)=\frac{Y}{4\pi}\int_S\frac{\Delta U}{(Z-\zeta)^2+Y^2}\left(1+\frac{X-\xi}{R}\right)dS$$

$$-\int_S\Psi\Delta V dS+\int_{\bar V}U^2\Psi_\xi\,d\bar V \tag{6}$$

where

$$\Psi=1/4\pi R \tag{7}$$

Here, S represents the wing planform area and $\bar V$ the total volume enclosed by the surface at infinity, the surface surrounding the singular point, the surface around any shock discontinuity, the wing surface, and the trailing vortex sheet.

The harmonic solution Φ_P for linearized subsonic theory can be written as

$$\Phi_P=-\int_S\Psi\Delta V_P dS+\frac{Y}{4\pi}\int_S\frac{\Delta U_P}{Y^2+(Z-\zeta)^2}\left(1+\frac{X-\xi}{R}\right)dS \tag{8}$$

Φ_P satisfies the same boundary conditions as Φ corresponding to the nonlinear theory. So, according to the thin airfoil theory

$$\Delta\Phi_Y(X,0,Z)=\Delta\Phi_{PY}(X,0,Z),\quad 0\le X\le 1 \tag{9}$$

Since the integral over S in Eqs. (6) and (8) means integration over only the wing planform, the second term on the right-hand side of Eq. (6) equals to the first term of the right-hand side of Eq. (8), in view of Eq. (9).

The subtracting Eq. (8) from Eq. (6) follows

$$\Phi(X,Y,Z)=\Phi_P(X,Y,Z)+\frac{Y}{4\pi}\int_S\frac{\Delta U-\Delta U_P}{Y^2-(Z-\zeta)^2}$$

$$\times\left(1+\frac{X-\xi}{R}\right)dS+I'(X,Y,Z;U) \tag{10}$$

where

$$I'(X,Y,Z;U)=\int_{\bar V}U^2\Psi_\xi\,d\bar V$$

Differentiating Eq. (10) with respect to X gives

$$U(X,Y,Z)=U_P(X,Y,Z)$$

$$+\frac{Y}{4\pi}\int_S\frac{\Delta U(\xi,0,\zeta)-\Delta U_P(\xi,0,\zeta)}{[(X-\xi)^2+Y^2+(Z-\zeta)^2]^{3/2}}dS+\frac{\partial I'}{\partial X} \tag{11}$$

Now, taking limits as $Y\to\pm 0$ and considering the second term on the right-hand side of Eq. (11) as the well-known Poisson's integral, it follows for continuous flow that

$$U(X,\pm 0,Z)=U_P(X,\pm 0,Z)\pm\tfrac{1}{2}[\Delta U(X,0,Z)$$

$$-\Delta U_P(X,0,Z)]+\lim_{Y\to\pm 0}(\partial I'/\partial X) \tag{12}$$

If there is no shock discontinuity, it can be shown[1] by integrating $I(X,Y,Z,U)$ by parts in the X direction that $I(X,Y,Z,U)=I'(X,Y,Z,U)$, and so the Nörstrud's integral Eqs. (1) result. If there is a shock discontinuity, then integrating by parts in the X direction $I(X,Y,Z,U)$ gives

$$I(X,Y,Z,U)=-\int_{\text{shock}}\Psi[U^2]\cos\sigma_1 dS+I'(X,Y,Z;U) \tag{13}$$

where the upstream unit normal to the shock surface has been taken as

$$\bar n=i\cos\sigma_1+j\cos\sigma_2+K\cos\sigma_3$$

Now, the first term on the right-hand side of Eq. (13) along with the integral terms over the shock surface which appeared in the course of formulating Eq. (6) give no contribution because of the small disturbance approximation of shock jump conditions.[1] Thus, Eq. (11) as well as Eq. (12) is valid, for the piecewise continuous function $\Delta U(X,Y,Z)$ on the boundary $Y=0$, even for the case when shock discontinuity appears.

Acknowledgment

The author takes this opportunity to thank P. Niyogi of Jadavpur University and B. C. Basu for their continuous encouragement and valuable suggestions while preparing this Note.

References

[1] Klunker, E. B., "Contribution to Methods for Calculating the Flow about Thin Lifting Wings at Transonic Speeds—Analytic Expressions for the Far Field," NASA TND-6530, Nov. 1971.

[2] Ferrari, C. and Tricomi, F. G., *Transonic Aerodynamics*, Academic Press, New York, 1968, Chap. VI, Sec. 10.1.

[3] Nörstrud, H., "High Speed Flow Past Wings," NASA CR-2246, April 1973.

[4] Niyogi, P., "Transonic Integral Equation for Lifting Profiles and Wings," *AIAA Journal*, Vol. 16, Jan. 1978, pp. 92-94.

[5] Nörstrud, H., "Numerische Lösungen für Schallnahe Strömungen um Ebene Profile," *Zeitschrift für Flugwissenschaften*, Vol. 18, Sept. 1970, pp. 149-157.

[6] Epstein, B., *Partial Differential Equations*, McGraw Hill Inc., New York, 1962, Chap. 6, Article 12.

Calculation of Two-Dimensional Turbulent Boundary Layers

Sedat Biringen* and Josef Levi†
Bogazici University, Bebek, Istanbul, Turkey

Introduction

IN this Note, the boundary layer over a flat plate is calculated with a three-equation model of turbulence which makes use of transport equations for the kinetic energy k, the

Received Dec. 27, 1977; revision received April 20, 1978.

Index categories: Boundary Layers and Convective Heat Transfer—Turbulent; Computational Methods.

*Assistant Professor; also Post-Doctoral Scholar, Mechanical Engineering Dept., Stanford University, Stanford, Calif.

†Graduate Student.

shear stress $\overline{uv}$, and an integral length scale L. The basic objective stems from an earlier work[1] in which the same system of equations was used to calculate axisymmetric wakes and coflowing jets. Diffusion terms in the governing equations were modeled by Bradshaw's[2] bulk convection hypothesis, and the resulting hyperbolic system of equations was solved by the explicit, two-level Lax-Wendroff finite-difference scheme. Results indicated an anomalous behavior of the k profiles in regions close to the symmetry axis. This was attributed to the fact that the necessary number of boundary conditions specified on the centerline exceeded the number of ingoing characteristics, hence altering the well-posed character of the differential equations in a narrow region around the centerline. Here an alternative approach to model the diffusion terms is adopted. The bulk convection formulation is modified by employing terms involving second-order differentials of k, $\overline{uv}$, and L. This makes the governing system of equations of the parabolic type; hence the number of allowable conditions at the inner boundary no longer is restricted by the number of ingoing characteristics. In order to investigate the effect of second-order terms, which represent gradient diffusion, a parametric study is made by setting the coefficients in front of the second-order terms to zero and then progressively increasing them.

Governing Equations

The governing equations are written with respect to Cartesian coordinates x, y, z. The mean velocity components are U, V, W, and the fluctuating velocity components are u, v, w, respectively. An overbar denotes a time average, a repeated index indicates summation, and subscript e refers to freestream conditions. The flow is assumed to be steady, two-dimensional, incompressible and have constant properties. The governing equations are simplified by the boundary-layer approximations. Closure assumptions for higher order terms that appear in the k, $\overline{uv}$, and L equations have been made following Refs. 2-4; the details are given in Ref. 5. The expression used to model the diffusion terms in the governing equations reads[1]

$$\overline{\theta' u_i} = C(V_\theta)_i \bar{\theta} + C' u_t L_t \frac{\partial \bar{\theta}}{\partial x_i} \tag{1}$$

where θ is the diffused quantity, C and C' are empirical constants, $(V_\theta)_i$ is a turbulent transport velocity characteristic of large-scale motion, and u_t and L_t are the characteristic velocity and length scales of the turbulence, respectively. Assuming that $u_t \sim k^{1/2}$ and $L_t \sim L$ and merging C into $(V_\theta)_i$, one obtains, for the diffusion terms in the k and $\overline{uv}$ equations,

$$\overline{kv} = V_k k + \alpha k^{1/2} L \frac{\partial k}{\partial y} \tag{2a}$$

$$\overline{uv^2} = V_j \overline{uv} + \beta k^{1/2} L \frac{\partial \overline{uv}}{\partial y} \tag{2b}$$

The bulk velocities V_j and V_k have been estimated following Refs. 1 and 2 and read

$$V_k = (\overline{uv})^{1/2}_{\max} f_1(y), \quad V_j = (\overline{uv})^{1/2}_{\max} f_2(y)$$

where $f_1(y)$ and $f_2(y)$ are functions to be determined empirically. The function $f_1(y)$ was evaluated from the empirical bulk velocity data of Bradshaw and Unsworth[6] for $\overline{kv}/\overline{uv}$ by transforming it into an empirical function for $\overline{kv}/k$, assuming that $\overline{uv} \sim k$ (Fig. 1). Following Ref. 1, $f_2(y)$ was taken to be equal to $f_1(y)$, and no further adjustments were made to the empirical inputs once they were prescribed as defined previously. The length scale is obtained by simplifying a rate equation given by Rotta.[1,3]

Approximate forms of the governing equations then are written in the following general form:

$$\frac{\partial \tilde{f}}{\partial \tilde{x}} + \tilde{A}\frac{\partial \tilde{f}}{\partial \eta} + \tilde{B}\frac{\partial^2 \tilde{f}}{\partial \eta^2} + \tilde{C} = 0 \tag{3}$$

where

$$\tilde{f} = \begin{bmatrix} \tilde{U} \\ \tilde{k} \\ \tilde{\overline{uv}} \\ \tilde{L} \end{bmatrix}$$

$$\tilde{C} = \frac{1}{\tilde{U}} \times \begin{bmatrix} -\tilde{U}_e \left(\dfrac{d\tilde{U}_e}{d\tilde{x}}\right) \\ \left(\dfrac{\partial \tilde{V}_k}{\partial \eta}\right)\dfrac{\tilde{k}}{\tilde{\delta}} + C_D \dfrac{\tilde{k}^{3/2}}{\tilde{L}} \\ \left[\left(\dfrac{\partial \tilde{V}_J}{\partial \eta}\right)\dfrac{1}{\tilde{\delta}} + C_{\phi 1} C_D \dfrac{\tilde{k}^{1/2}}{\tilde{L}}\right]\tilde{\overline{uv}} \\ C_D (C_8 - 1)\tilde{k}^{1/2} \end{bmatrix}$$

$$\tilde{A} = \frac{1}{\tilde{U}\tilde{\delta}} \begin{bmatrix} \tilde{V} & 0 & 1 & 0 \\ \tilde{\overline{uv}} & (\tilde{V}+\tilde{V}_k) & 0 & 0 \\ \tilde{k}(C_2 - C_{\phi 2}) & 0 & (\tilde{V}+\tilde{V}_J) & 0 \\ \dfrac{\tilde{\overline{uv}}\tilde{L}}{\tilde{k}}(C_6 - 1) & 0 & 0 & (\tilde{V}+\tilde{V}_k) \end{bmatrix}$$

$$\tilde{B} = \frac{1}{\tilde{U}\tilde{\delta}} \begin{bmatrix} 0 & 0 & 0 & 0 \\ 0 & \alpha\tilde{k}^{1/2}\tilde{L} & 0 & 0 \\ 0 & 0 & \beta\tilde{k}^{1/2}\tilde{L} & 0 \\ 0 & 0 & 0 & \gamma\tilde{k}^{1/2}\tilde{L} \end{bmatrix}$$

Here, a tilde denotes a nondimensional quantity, γ is the constant that appears in front of the second-order (gradient diffusion) term in the modeled L equation, and η is the cross-stream coordinate nondimensionalized by the boundary-layer thickness δ. Because of the slow increase of δ with $\tilde{x}$, this transformation maps the integration domain into an almost rectangular one. In deriving Eq. (3), second-degree terms like $(\partial k/\partial y)^2$ and $(\partial k/\partial y)(\partial L/\partial y)$ have been neglected, and, from the limiting forms of Eq. (3), one obtains $(C_2 - C_{\phi 2}) = C_{\phi 1} C_D$ and $C_8 = C_6$ as restrictions in choosing the model constants. The various constants that appear in Eq. (3) are summarized in Table 1. The cross-stream mean velocity $\tilde{V}$ appears only in the coefficient matrix $\tilde{A}$ and hence can be calculated separately from the equation along the vertical characteristic. This is obtained from the x-momentum equation via the equation of continuity and reads

$$\frac{d\tilde{V}}{d\eta} - \frac{\tilde{V}}{\tilde{U}}\frac{d\tilde{U}}{d\eta} + \frac{\tilde{U}_e \delta}{\tilde{U}}\frac{d\tilde{U}}{d\tilde{x}} - \frac{1}{\tilde{U}}\frac{d\tilde{\overline{uv}}}{d\eta} = 0 \tag{4}$$

It can be shown that when α, β, γ, and hence $\tilde{B}$ are set equal to zero, Eq. (3) will be a hyperbolic system.[1,5] For $|\alpha|$, $|\beta|$, and $|\gamma|$ greater than zero, the system will be parabolic, but for small $|\alpha|$, $|\beta|$, $|\gamma|$ (large ratios of convective to diffusive terms), Eq. (3) should be expected to exhibit a hyperbolic character.

Calculation Procedure

The "wall" boundary conditions are prescribed at the first mesh point away from the wall by using empirical formulas

Table 1 Turbulence model constants

Constant	Transport term	Evaluation	Value
C_D	k dissipation	Ref. 7	0.08
C	$\overline{uv}$ redistribution	Ref. 4	1.5
$(C_2 - C_{\phi 2})$	$\overline{uv}$ production	$C_{\phi 1} C_D$	0.12
C_6	L production	Ref. 3	0.8
C_8	L dissipation	C_6	0.8

via the law of the wall in the manner suggested in Ref. 7. At the freestream edge, $\tilde{U}$ is set equal to $\tilde{U}_e$, $\tilde{k}$ and $\widetilde{\overline{uv}}$ are set equal to zero, and the derivative with respect to η of $\tilde{L}$ is set to zero. The outer edge of the flow is taken as that point where the difference between two successive values of the mean velocity is less than a specified amount.[1,2] In order to integrate Eq. (3) with these boundary conditions, the three-level, explicit DuFort-Frankel method has been employed. Using this scheme, Eq. (3) can be put into the following finite-difference form (Fig. 2):

$$F_{i,j+1} = (\tilde{BI})_{i,j} \times F_{i,j} - \frac{\Delta x}{\Delta \eta} (\tilde{BI})_{i,j} \times \tilde{A}_{i,j} (F_{i+1,j} - F_{i-1,j})$$

$$- r(\tilde{BI})_{i,j} \times \tilde{B}_{i,j} (F_{i+1,j} - F_{i,j-1} + F_{i-1,j}) - 2(\Delta \tilde{x})(\tilde{BI})_{i,j} (\tilde{C})_{i,j} \tag{5}$$

where $r = 2\Delta \tilde{x}/\Delta \eta^2$, $\tilde{BI} = (I - r\tilde{B})^{-1}$, I is the identity matrix, and F is the finite-difference approximation to $\tilde{f}$. It can be shown that the DuFort-Frankel scheme is stable in the von Neumann sense if the Courant number is less than one. Hence, all through the calculations, the Courant-Friedrichs-Lewy (CFL) condition was obeyed in choosing the step size in the marching direction. According to this,

$$\Delta \tilde{x} = F_a (\Delta \eta / \lambda_{\max})$$

where $\lambda_{\max}$ is the largest eigenvalue of $\tilde{A}$, and F_a is a safety factor less than one. The safety factor F_a was kept sufficiently small to meet the stability requirements of the DuFort-Frankel representations of the quasilinear convection-diffusion type of equations.[8] It should be noted that the foregoing scheme reduces to the leapfrog scheme when $\tilde{B}$ is set equal to zero. The stability requirement for this case is the same as in the foregoing.

Equation (5) was solved by a Fortran program on a Univac 1106 computer. The details of the program are given in Ref. 5. Initial conditions for the unknowns $\tilde{U}$, $\tilde{k}$, $\widetilde{\overline{uv}}$, and $\tilde{L}$ were generated in the manner suggested in Ref. 7. Calculations were performed for the boundary layer in a zero pressure gradient assuming that this would be adequate both to investigate the stability of the hyperbolic problem and to test partially the

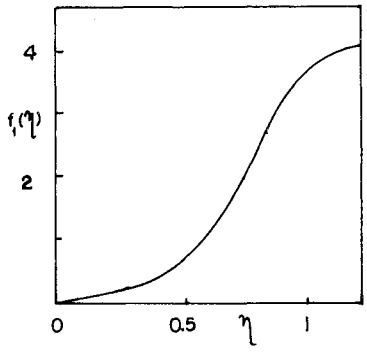

Fig. 1 Empirical function $f_1(\eta)$.

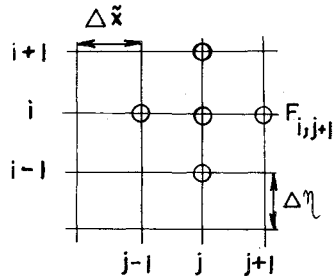

Fig. 2 DuFort-Frankel computational molecule.

capabilities of the model. Calculations were performed at first by setting α, β, and γ equal to zero. In spite of the fact that the CFL condition was obeyed, results indicated the existence of oscillations on the kinetic energy and the shear stress profiles close to the solid wall after a few steps in the integration procedure. Repeated calculations with smaller step sizes in the marching direction did not reveal any appreciable improvements in the results. However, increasing values of the parameters acted to damp the oscillations, and the values of $|\alpha| = 3$, $|\beta| = 3$, $|\gamma| = 0.01$ were found to be adequate to restore stability. It should be noted that these values of $|\alpha|$ and $|\beta|$ fall within the range of gradient diffusion model constants of the triple velocity correlations reported in the literature.[4] These values are also much larger than those values of "numerical dissipation term" coefficients, which are sometimes added to center-differenced finite-difference representations of hyperbolic equations. Hence, they should be accepted as evidence that inclusion of gradient diffusion terms has a stabilizing effect on the solution and that the gradient diffusion process should be represented in the modeled diffusion terms to have numerical stability.

A comparison of the predicted $\tilde{U}$, $\tilde{k}$, and $\widetilde{\overline{uv}}$ profiles with other predictions[4,6] and experimental results[9] is shown in Fig. 3. The $\tilde{U}$ profile is in excellent agreement with experimental results, and good agreement is obtained for the $\tilde{k}$ and $\widetilde{\overline{uv}}$ profiles. In Fig. 4, the boundary-layer integral parameters, the

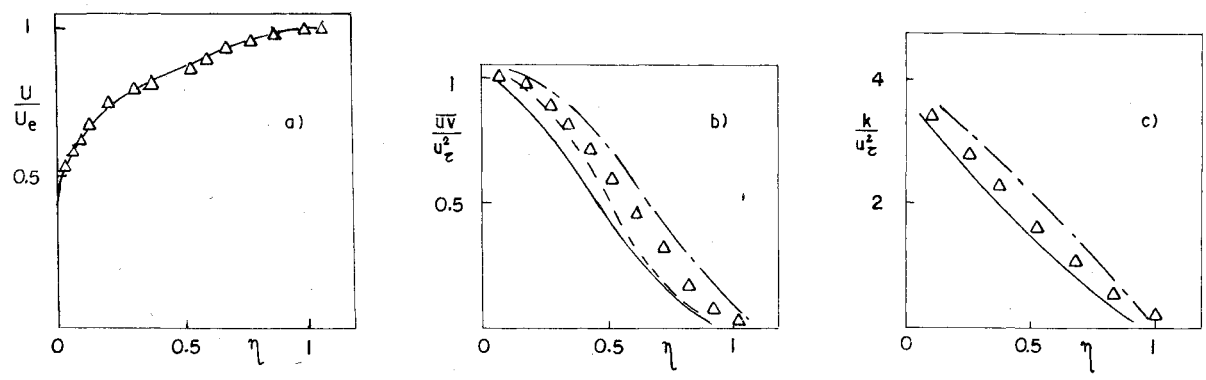

Fig. 3 a) U profile, b) uv profile, and c) k profile at $\tilde{x} = 30$; $|\alpha| = 3$, $|\beta| = 3$, $|\gamma| = 0.01$; ——, present predictions; --, Ref. 6; – –, Ref. 4; Δ, Ref. 9.

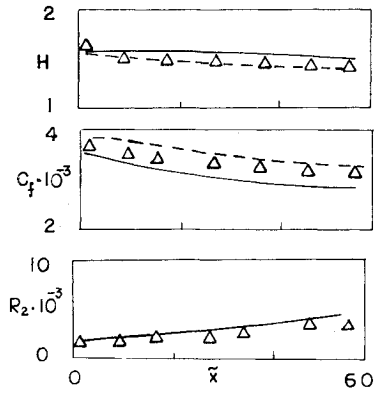

Fig. 4 Integral parameters of the boundary layer; $|\alpha| = 3$, $|\beta| = 3$, $|\gamma| = 0.01$; —, present predictions; --, Ref. 6; Δ, Ref. 9.

shape factor H, friction coefficient C_f, and the momentum thickness Reynolds number are shown as functions of the streamwise coordinate $\tilde{x}$. The shape factor remains almost constant, whereas the friction coefficient is slightly underpredicted.

Summary

The main features of this work are summarized as follows.

1) With the inclusion of second-order (gradient diffusion) terms for $\tilde{k}$, $\widetilde{uv}$, and $\tilde{L}$, the method is capable of predicting closely the mean flow as well as the turbulent characteristics of the flat-plate boundary layer.

2) In the case when $|\alpha|$, $|\beta|$, and $|\gamma|$ are greater than zero, stability is restored because of the condition that $\tilde{k}$, $\widetilde{uv}$, and $\tilde{L}$ appear under second-order derivatives, and the system of equations becomes parabolic. This supports the earlier idea that for the hyperbolic set of equations the well-posed character of the differential equations is altered in a region close to the inner boundary.[1]

3) The restoration of numerical stability for $|\alpha|$, $|\beta|$, and $|\gamma|$ greater than zero and the values that they assume suggest that gradient diffusion should be accounted for at least close to the inner boundary.

Acknowledgment

The authors would like to thank J. H. Ferziger of Stanford University for his comments on the earlier manuscript of this paper.

References

[1] Biringen, S., "Calculation of Axisymmetric Jets and Wakes with a Three-Equation Model of Turbulence," *Journal of Fluid Mechanics* (in press).

[2] Bradshaw, P., Ferriss, D. H., and Atwell, N. P., "Calculation of Boundary Layer Development Using the Turbulent Energy Equation," *Journal of Fluid Mechanics*, Vol. 28, March 1967, pp. 593-616.

[3] Rotta, J., "Recent Attempts to Develope a Generally Applicable Calculation Method for Turbulent Shear Flow Layers," *Conference Proceedings No. 93 on Turbulent Shear Flows*, AGARD CP-93, Paper A-1, 1971.

[4] Hanjalic, K. and Launder, B. E., "A Reynolds Stress Model of Turbulence and Its Application to Thin Shear Flows," *Journal of Fluid Mechanics*, Vol. 52, April 1972, pp. 609-683.

[5] Levy, J., "Calculation of the Boundary Layer over a Flat Plate with a Three-Equation Model of Turbulence," M.S. Thesis, Mechanical Engineering Dept., Bogazici Univ., Istanbul, Turkey, 1977.

[6] Bradshaw, P. and Unsworth, K., "An Improved Fortran Program for the Bradshaw-Ferriss-Atwell Method of Calculating Turbulent Shear Layers," Imperical College, London, I.C. Aero-Rept. 74-02, 1974.

[7] Ng, K. H. and Spalding, D. B., "Predictions of Two-Dimensional Boundary Layers on Smooth Walls with a Two-Equation Model of Turbulence," *International Journal of Heat and Mass Transfer*, Vol. 19, 1976, pp. 1161-1172.

[8] Roache, P., *Computational Fluid Dynamics*, 1st ed., Hermosa Publishers, Albuquerque, N. Mex., 1972, pp. 61-64.

[9] Klebanoff, P. S., "Characteristics of Turbulence in a Boundary Layer with Zero Pressure Gradient," NACA Rept. 1247, 1955.

Generalized Area Rules and Integral Theorems for Hypersonic Wing-Bodies

N. D. Malmuth*
Science Center, Rockwell International, Thousand Oaks, Calif.

Introduction

THE advent of modern shock-capturing techniques has led to nonlinear flow solutions for complex configurations such as the Shuttle Orbiter. A description of a typical implementation is discussed in Ref. 1. Recent interest in hypersonic transport and scramjet vehicles employing favorable interference as well as high-acceleration missiles has stimulated the need for increased understanding of the parametric dependencies in such flows. Generally, these relationships are not readily accessible from computer solutions. In particular, the compression lift on flat-top-wing-body combinations provides a basis for obtaining high aerodynamic efficiencies. Analytical results are required to clarify the geometrical relationships necessary to optimize these benefits.

In Ref. 2, an area rule was obtained for the change in L/D of a hypersonic delta wing due to the addition on its compressive side of a conical body of arbitrary cross section. The body was considered *conically subsonic*, and the details of the pressure field over that configuration were quantified in Ref. 3. In this Note, the appropriate relationships will be obtained for a *nonconical* body and a *conically supersonic* conical shape. Finally, area progressions will be derived optimizing L/D for the nonconical class of configurations.

Nonconical Flows

Figure 1 depicts a nonconical body $OABA'$ on the compressive side of a hypersonic delta wing OCC' in the plane $\bar{y}=0$. The equation of the body is $\bar{y}=\epsilon\delta f(\bar{x},\bar{z})$, $-z_B \le z \le z_B(\bar{x})$, where $z=\pm z_B(x)$ are the "ridge line" curves OA and OA', and f is a continuous single-valued function with $f(\bar{x},\pm z_B)=0$.

The wing-body is assumed to be weakly three dimensional in the sense indicated in Ref. 2, through a limit involving the sweepback angle χ. The nonconical problem for the pressure perturbation about the freestream field is hyperbolic, and the domain of dependence of the body depends on whether $z_B(\bar{x})$ is time-like or space-like[4] or correspondingly subsonic or supersonic in the sense that the component of the local Mach number normal to the edge is subsonic or supersonic. Associated with the former case, $z_B'(\bar{x}) < \tan\mu$, where μ, the local Mach angle, is given by $\sin^{-1} c\delta$, and $c^2=\gamma(\gamma-1)/2$, where γ is the specific heat ratio.† For supersonic edges, the inequality is reversed. The nonconical results derived herein are restricted to the subsonic leading-edge case shown in Fig. 1, where the body is assumed to have a conical nose and the domain of dependence is the Mach cone $z^2=c^2x^2-y^2$ ($x=\bar{x}$, $y=\bar{y}/\delta$, $z=\bar{z}/\delta$). It is plausible that the results to be derived hold for the supersonic leading-edge case in which the domain of dependence is bounded by a characteristic envelope of Mach cones whose apices lie along OA and OA'. This conclusion relates to superposition procedures that can be used

Received Oct. 9, 1975; revision received June 21, 1978.

Index category: Supersonic and Hypersonic Flow.

*Project Manager, Fluid Dynamics. Associate Fellow AIAA.

†The freestream Mach number, M_∞, is assumed hereinafter infinite for convenience. Generalization to arbitrary hypersonic M_∞'s is straightforward.